Macromolecules
ARTICLE

Macromolecules **2009**, *42*, 4165–4174 **4165**
DOI: 10.1021/ma900077w

Dielectric Properties of Nanocomposites Based on Polyethylene and Layered Double Hydroxide

Andreas Schönhals,*,† Harald Goering,† Francis Reny Costa,‡,§ Udo Wagenknecht,‡ and Gert Heinrich‡

†*BAM Federal Institute for Materials Research and Testing, Unter den Eichen 87, 12200 Berlin, Germany, and* ‡*Leibniz Institute of Polymer Research, Hohe Strasse 6, 01069 Dresden, Germany.* §*Present address: Borealis Polyolefine GmbH, St.-Peterstrasse 25, 4021 Linz, Austria*

Received January 14, 2009; Revised Manuscript Received May 8, 2009

ABSTRACT: Nanocomposites with a predominantly exfoliated morphology were prepared by melt blending of organically modified doubled layered hydroxide (LDH) and low density polyethylene (PE). The prepared materials were investigated by differential scanning calorimetry (DSC) and in detail by dielectric spectroscopy. The DSC experiments show that the degree of crystallinity decreases linearly with increasing content of the LDH. The extrapolation of this dependence to zero results in a limiting concentration of ca. 50 wt % LDH were the crystallization of PE is completely suppressed by the nanofiller. The dielectric response of pure polyethylene shows different weak relaxation processes. The intensity of dynamic glass transition (β-relaxation) increases with the concentration of LDH. This is attributed to the increasing concentration of the exchanged anion dodecyl benzene sulfonate (SDBS). The SDBS molecules are strongly adsorbed at the exfoliated LDH layers. Therefore, a detailed analysis of the β-relaxation provides information about the structure and the molecular dynamics in the interfacial region between the exfoliated LDH layers and the polyethylene matrix. This analysis shows that the β-relaxation region consists of two processes: both of them obey glassy dynamics. The difference in corresponding Vogel (ideal glass transition) temperatures is about 30 K. The relaxation process at lower frequency is assigned to polyethylene segments with a reduced molecular mobility close to LDH layers. The process at higher frequencies is related to polyethylene segments in a farer distance for the surface of the nanofiller. In the nanocomposite materials an additional process due to Maxwell−Wagner−Sillars (MWS) polarization was observed. The time constant of this MWS process can be correlated with characteristic length scales in nanocomposites and therefore provides additional information on dispersion and delamination/exfoliation of the LDH layers in these materials.

1. Introduction

Over the past decade polymer-based nanocomposites gained rapidly increasing interest from the point of view of both basic and applied researches.[1−7] This is due to their favorable and often unique combination of properties. They show remarkable property improvements such as increased tensile properties, decreased gas permeability, decreased solvent uptake, increased thermal stability, and flame retardancy when compared to conventionally scaled composites. This is directly related to the small size of the filler particles and their dispersion on the nanometer scale. Besides this, the interface area between the nanoparticles and the polymer matrix is crucial for the properties of polymer-based nanocomposites. Because of the high surface to volume ratio of the nanoparticles the volume fraction of the interface area is high.[2,4,8] It is directly influenced by an adjacent nanoparticle surface. Moreover for nanosized filler particles the length scale of interaction corresponds to the size of several repeating units of the polymer chains which is smaller than in conventional scaled composite materials. In addition modifications in packing density and molecular mobility of the polymer segments in the interface area between nanoparticle and matrix are expected.[9−12] Despite a lot of experimental work available in the literature, there is a lack of even simple structure−property models. Without such models the progress in the field of nanocomposites remains largely empirical.[8]

Recently among other particles like layered silicates (clay),[1−7] nanosized metals,[13] carbon nanotubes,[14−16] or polyhedral oligomeric silsesquioxane[17−20] layered double hydroxides (LDH) are gaining increasing interest as nanofiller for polymer-based nanocomposites.[21−23] LDH materials have a broad range of chemical composition and are well-known for their catalytic activity.[24] Because of a large amount of tightly bounded water[25] and other synergistic effects, they are able to enhance the flame retardancy of polymer materials.[26,27] Like layered silicates, LDH materials have a crystalline geometry with a variety of interlayer anions, which can be exchanged by bulky organic anionic species. This makes LDH especially suitable to prepare polymer nanocomposites because macromolecules can intercalate into the gallery of organically modified LDH and result in the exfoliation of LDH layers.

Here the structure/property relationships of nanocomposites based on low density polyethylene and LDH are investigated mainly by dielectric spectroscopy. Recently dielectric spectroscopy has been successfully applied to a variety of polymer/clay nanocomposites.[12,28−31]

2. Experimental Section

LDH materials belong to the general class of anionic clay minerals. Their structures (and those of hydrotalcites in general)

*Corresponding author. Telephone +49 30/8104-3384. Fax: +49 30/8104-1637. E-mail: Andreas.Schoenhals@bam.de.

Published on Web 05/28/2009

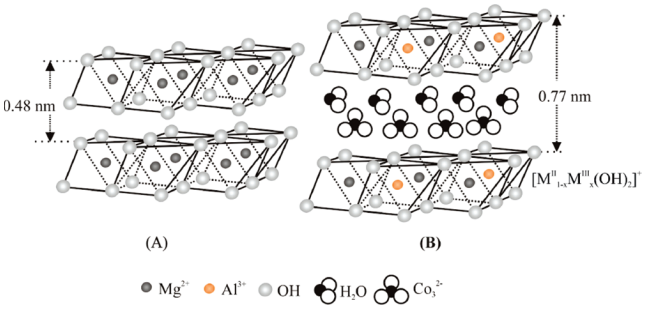

Figure 1. Schematic representation of layered structures: (A) brucite-like sheets; (B) LDH. The figure was adapted from ref 21.

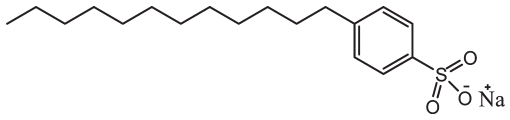

Figure 2. Chemical structure of dodecyl benzene sulfonate (SDBS).

are similar to that of brucite ($Mg(OH)_2$) where each magnesium cation is octahedrally surrounded by hydroxyl groups. An isomorphous substitution of Mg^{2+} by a trivalent cation or by a combination of trivalent and other divalent cations occurs in the LDHs. As a result, a positive charge is generated in the brucite sheet, which is otherwise electroneutral. The positive charge is compensated by anions in the interlayer. In these inter galleries strongly bonded water molecules also exist. A scheme of brucite and LDH is given in Figure 1. The LDHs are generally described by the formula $[M_{1-x}^{2+}M_x^{3+}(OH)_2]^{x+}(A^{z-})_{x/z}\cdot mH_2O$, where M^{2+} and M^{3+} are the metal cations. A^{z-} represents the anions to balance the positive charge of the layer. For the used LDH, the metal cations are Al^{3+} and Mg^{2+} (see Figure 1b) were the synthesis is described in detail in ref 22. In this point, it should be noted that LDH is quite different from layered silicates. For LDH each crystal layer is composed of a single octahedral metal hydroxide sheet whereas in layered silicates it is a sandwiched structure of two or more sheets of metal oxides. The inter gallery anions were exchanged by dodecyl benzene sulfonate (SDBS) whose chemical structure is given in Figure 2. Again details are given elsewhere.[21,22]

Low density polyethylene (LDPE; density 0.9225 g/cm^3; melt flow index MFI 3.52 g/10 min) was purchased from Exxon Mobil, Belgium. Maleic anhydride grafted polyethylene (MAH-*g*-PE) (density 0.926 g/cm^3, MFI 32.0 g/10 min, maleic anhydride concentration 1.0 wt %) was used as compatibilizer. It was obtained from Crompton, USA.

The nanocomposites were prepared by melt mixing in a twin-screw extruder (27 mm screw diameter, L/D ratio 36, 160−200 °C temperature profile from the feed to the extruder barrel, 200 rpm screw speed and 6 kg h^{-1} feed rate) applying a two step procedure. In the first step a master batch (containing the filler and compatibilizer) was prepared from SDBS modified LDH and MAH-*g*-PE in a ratio 1:2 (weight). In the second step the masterbatch was added in the selected concentration to the base LDPE and compounded in the same extruder using the same conditions for the preparation of the masterbatch. Further information of the preparation of the composites can be found together with a structural and rheological characterization elsewhere.[21] Details of the prepared samples are listed in Table 1. The nominal weight fraction of LDH is measured by its metal hydroxide content. TEM images show many well exfoliated LDH sheets besides a few larger LDH particles.[21−23] So, the nanocomposites have a predominantly exfoliated morphology. A model for the exfoliation mechanism is presented in ref 21.

Dielectric relaxation spectroscopy was applied to investigate the molecular mobility of the nanocomposites. For polymers this method is sensitive to fluctuations of dipoles which are related to the molecular mobility of groups, segments or the polymer chain

Table 1. Code and Composition of the Investigated Nanocomposites[a]

code	c_{LDH} [wt %]	T_{Melt} [K]	ΔH_{Melt} [J/g]	ΔH_{Cryst} [J/g]
PE	0	379.0	190	−179
MAH-*g*-PE	0	392.7		
	0			
PELDH1	2.43	378.7	182	−178
PELDH2	4.72	379.0	179	−177
PELDH3	6.89	379.3	172	−166
PELDH4	8.94	379.7	169	−168
PELDH5	12.73	380.0	154	−154
PELDH6	16.20	380.7	153	−151

[a] In addition the melting temperature T_{Melt}, the melting enthalpy ΔH_{Melt} (second heating run), and the crystallization enthalpy ΔH_{Cryst} (first cooling run) are given.

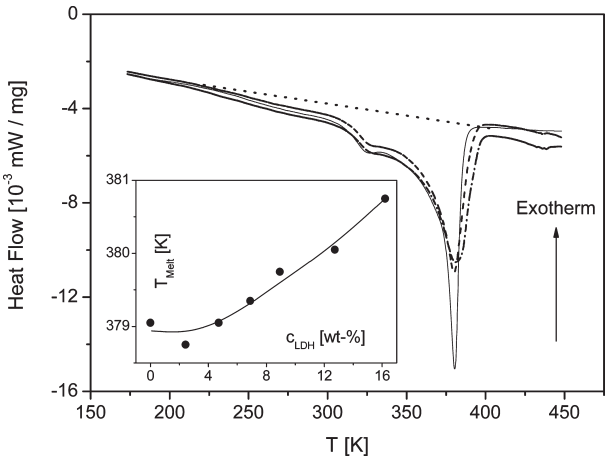

Figure 3. DSC curves for PE and corresponding nanocomposites (first heating run): solid line, PE; dashed line, 8.94 wt % LDH; dashed−dotted line, 16.2 wt % LDH. The dotted line indicates the temperature range used for the estimation of melting enthalpy. The inset gives the dependence of T_{Melt} on the concentration of LDH. The line is a guide for the eyes.

as well. Fundamental details are given elsewhere.[32] The sample is placed between two gold covered stainless steel electrodes in parallel plate geometry (diameter 20 mm). The complex dielectric function $\varepsilon^*(f) = \varepsilon'(f) - i\varepsilon''(f)$ (f = frequency; ε' and ε'' = real and imaginary part of the complex dielectric function, $i = -1^{1/2}$) is isothermally measured in the frequency range from 10^{-1} to 10^7 Hz by a high resolution ALPHA analyzer (Novocontrol). The temperature of the sample is controlled by a Quatro Novocontrol cryo-system with a stability better than 0.1 K. The temperature was varied from 173 to 413 K. A detailed description of the dielectric equipment used can be found in ref 33.

Thermal analysis was carried out by differential scanning calorimetry (DSC, Seiko instruments). The samples were measured from 173 to 473 K with a heating and cooling rate of 10 K/min. N_2 was used as protection gas. For each sample three heating and two cooling processes were measured. The enthalpy changes related to melting and heating were calculated from 225 to 480 K.

3. Results and Discussion

Figure 3 compares the DSC curves from the first heating run for LDPE, PELDH4 (8.94 wt %), and PELDH6 (16.2 wt %). All materials behave in a similar manner. No glass transition phenomena can be detected as it is expected for low density semicrystalline polyethylene.[34] A detailed discussion of crystallization and melting behavior of low density polyethylene including copolymers can be found elsewhere.[35,36] For the materials under study around 333 K, a pretransition phenomenon takes place which disappears after the first cooling run. Probably, it is related to the preparation of the samples or to its storage at room temperature. At higher temperatures, the broad melting

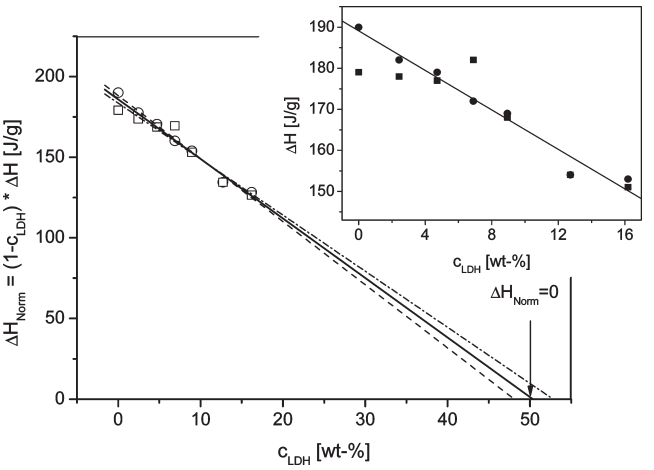

Figure 4. Melting (○, seconded heating) and crystallization (□, first cooling, positive values to have a common figure) enthalpies reduced to the content of the polymer vs the concentration of LDH. The dashed line is a linear regression using the data of the melting enthalpy. The dashed-dotted line is a linear regression using the data of the crystallization enthalpy. The solid is a linear regression using both data sets. The inset gives the melting (●) and crystallization (■) enthalpies versus the concentration of LDH. The line is a guide for the eyes.

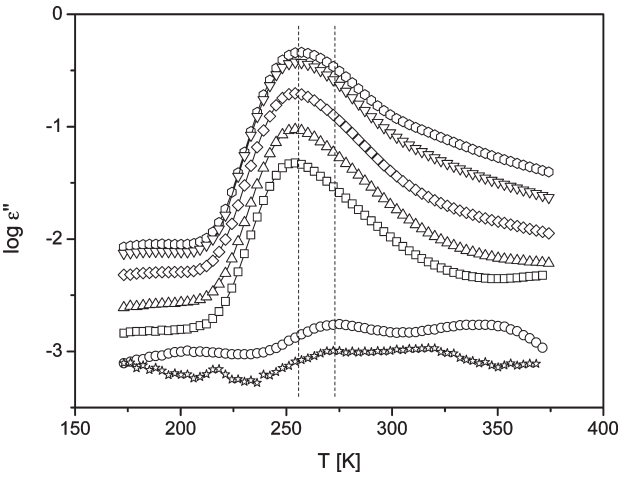

Figure 5. Dielectric loss ε'' versus temperature T at a frequency of 1 kHz for PE and different nanocomposites: (☆) polyethylene; (○) MAH-*g*-PE; (□) 2.43 wt % LDH; (Δ) 4.72 wt % LDH; (◇) 8.94 wt % LDH; (▽) 12.73 wt % LDH; (⬡) 16.2 wt % LDH.

transition with a peak at $T_{Melt} \approx 379$ K takes place. With increasing content of LDH, T_{Melt} shifts slightly to higher temperatures. This can be understood taking into consideration that with increasing LDH content also the mass fraction of MAH-*g*-PE increases, the latter has a higher melting temperature than PE (see Table 1). The second heating runes gave similar results with regard to the crystallization and melting enthalpies as well as the phase transition temperatures. In the inset of Figure 4 the dependence of the melting ΔH_{Melt} and crystallization enthalpy ΔH_{Cryst} is plotted versus the concentration of LDH. As expected both quantities decreases with increasing LDH concentration because the amount of the polymer in the sample decreases with increasing LDH content. However, ΔH also normalized to the content of the polymer (ΔH_{Norm}) decreases linearly with the concentration of LDH (see Figure 4). A similar dependence is obtained for heating and cooling. This means that the degree of crystallization (or the number of crystallites) decreases with the content of LDH. The extrapolation of ΔH_{Norm} to zero results in a critical concentration of LDH of ca. 50 wt %. For higher concentrations of the nanoparticels than this critical value no crystallization of PE can take place anymore. Probably, the nanoparticles act as defects and hinder the crystallization of the PE segments. The same was observed for nanocomposites based on polyamide.[37] Unfortunately this critical concentration of 50 wt % cannot be verified directly because no sample with such a high concentration of LDH can be prepared.

In this context, one has to note that for other systems an increase of the crystallization rate and also an more perfect crystals are observed for low concentrations of the nanofiller because the nanoparticles can act as additional nucleation sites.[38,39] Obviously the question whether nanofillers increase or decrease crystallization depends on the details of the system studied.

Upon studying the dielectric behavior of polyethylene (or other polymers with a high degree of crystallinity in general), it should be noted that the nomenclature of relaxation processes is different from that of amorphous polymers.[32] Figure 5 gives an overview about the dielectric behavior of the nanocomposites where the dielectric loss is plotted as a function of temperature for a fixed frequency of 1 kHz. The dielectric response of pure polyethylene is small because its repeating unit carries no intrinsic dipole moment. The weak dielectric losses are due to the presence of impurities in PE. Moreover by oxidation processes a small number of polar carbonyl groups can be formed.[32,40] Titanium dioxide was applied to control the oxidation without appreciable change in crystallinity.[41] Recently, the dielectric probe technique was also used to study the molecular dynamics of polyolefins in detail.[42]

The isochronal spectra of pure PE shows several weak relaxation processes indicated by peaks in the dielectric loss.[40]

The process located at ca. 275 K corresponds to the so-called β-relaxation in semicrystalline polyolefins, which is related to segmental fluctuations in the amorphous regions of PE (glassy dynamics, dynamic glass transition).[40] The dielectric loss of MAH-*g*-PE is slightly higher than that of pure PE but still weak due to the low concentration of the polar anhydride group. Like PE, MAH-*g*-PE shows a β-relaxation at around 275 K related to glassy dynamics. At higher temperature the so-called α-relaxation (or α_c-relaxation) is observed which assigned to the crystalline lamella. Its molecular nature is still under discussion. Probably this process is due to a rotational-translation of chain segments assisted by a chain twisting.[43−45] Moreover at lower temperatures than 275 K a further relaxation process (γ-relaxation) is observed which corresponds to localized fluctuations within the amorphous regions.[46] In the following the dielectric processes observed are discussed in their dependence on the concentration of LDH. The dynamic glass transition (β-relaxation) is addressed first, followed by an analysis of the γ-relaxation. Finally an additional observed interfacial polarization process is analyzed in detail in the context of the dispersion of the nanofiller.

Dynamic Glass Transition (β-Relaxation). For the nanocomposites the dielectric loss of the β-relaxation increases strongly with increasing concentration of LDH (see Figure 5). The polar component in the system which increases with the concentration of LDH is the bulky anion dodecyl benzene sulfonate (SDBS).[21] In the current understanding of nanocomposites with layered nanofillers it is assumed that the alkyl tail of the surfactant is desorbed from the surface of the layers and forms a common phase with the segments of the polymer. Therefore these polar molecules fluctuating together with the apolar polyethylene segments and monitor the molecular mobility of the latter. Therefore with increasing LDH concentration, this means with increasing SDBS concentration, the dielectric loss of the β-relaxation increases. This corresponds to a dielectric probe technique[42,47] but in difference to its conventional

applications here the location of the dielectric probe is known. Because of the strong negative charge of the SDBS this molecule is located predominantly close or adsorbed at the positively charged LDH layers. Therefore dielectric spectroscopy here probes selectively the molecular dynamics in an interfacial region close to the exfoliated LDH sheets because the dielectric loss of the polyethylene is low and so the matrix of the nanocomposite is nearly dielectrically invisible. Note that the dielectric loss of pure polyethylene is more than 1.5 orders of magnitude lower than that of the nanocomposite with the lowest concentration of LDH. A detailed analysis of the measured dielectric properties provides information about the structure and the molecular dynamic in this interfacial region. In the line of this argumentation, it would be interesting to investigate a sample of PE with SDBS without LDH. Unfortunately, no stable sample of this kind could be prepared even for low concentrations of SDBS because the surfactant molecules migrate to the surface of the specimen. This proves once again that the SDBS molecules are adsorbed onto the LDH sheets and that they are not free in the PE matrix.

In addition to the increase of the dielectric loss for the nanocomposites the β-relaxation is shifted to lower temperatures. This leads to the conclusion, that the molecular mobility in the interfacial region is higher than that in the bulk unfilled PE. Moreover, compared to conventional polymers the shape of the loss peak for the nanocomposites is quite unusual with a pronounced high temperature contribution.[48]

To further analyze of the isothermal data in the temperature region of the β-relaxation a derivative method is applied as suggested by van Turnhout and Wübbenhorst.[49,50] As example for a Debye-like relaxation process $\varepsilon''_{\mathrm{Deriv}} = -\mathrm{d}\varepsilon'/\mathrm{d}(\log f) = \varepsilon''^2$ holds. Because of the square in that formula a relaxation process appears narrower in $\varepsilon''_{\mathrm{Deriv}}$ than the corresponding peak in ε''. Therefore strongly overlapping broad relaxation peaks are better resolved. This is further supported by the fact that the discussed derivative can be regarded as the simplest approximation of the relaxation time spectrum which is a δ function for the Debye process.[50] The generalization of this approach to broadened relaxation processes (non-Debye response) observed here is discussed in detail in ref 50. Figure 6 displays $\varepsilon''_{\mathrm{Deriv}}$ versus frequency for the sample PELDH6 (16.2 wt %) at two temperatures. The spectra show a double peak structure. The same behavior is observed for all concentration of LDH in the nanocomposites. This means that the β-relaxation of the nanocomposites consist of at least two relaxation processes. For pure LDPE only a single relaxation process with a normal shape is found.[41,42]

The observed two relaxation processes are assigned to two different regions of molecular mobility of the polyethylene segments depending on the distance from the LDH particle surface which will be discussed below. There are only few papers that consider the structure and the dynamics of surfactant molecules intercalated within clay galleries (see for instance refs 51 and 52 and the literature quoted there) by NMR and dielectric spectroscopy or for lecithin molecules adsorbed on Aluminum oxide (Anopore).[53] These studies show that the polar headgroup is strongly adsorbed at the clay layers. The alkyl tails are partly collapsed on the silica sheets, but the surfactants have a certain molecular mobility which depends strongly on temperature.[51] Room temperature NMR studies show that the disorder and relaxation rates increase if the methyl terminus of the surfactant is approached.[51,52] In the presence of most

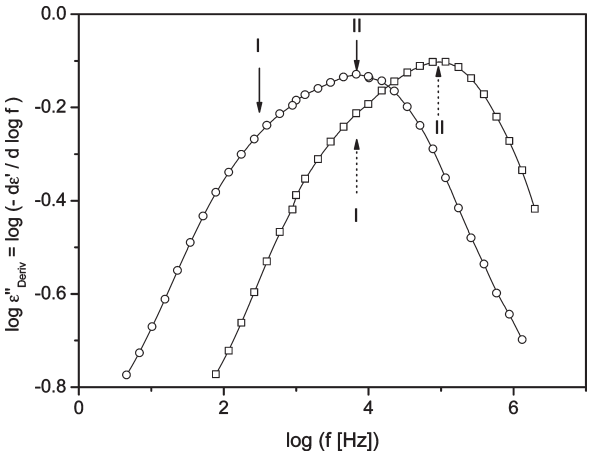

Figure 6. $\varepsilon''_{\mathrm{Deriv}} = -\mathrm{d}\varepsilon'/\mathrm{d}(\log f)$ versus frequency for PELDH6 (16.2 wt %): (○) 263.2 K; (□) 278.2 K. Lines are guides for the eyes.

intercalates, for instance, polymers the alkyl tails of the surfactant are desorbed from the surface of the silica sheet, extended to the interlayer and forms a mixed phase with the segments of the polymers. For the system under investigation, the same is assumed. The polar headgroup of the SDBS molecules interacts strongly with the surface of the LDH sheets and the polyethylene segments form a single phase with the alkyl tails of the surfactant. In a short distance the molecular mobility of this phase is decreased as discussed above. Therefore the low frequency process (process I) is assigned to the polyethylene segments and alkyl segments of SDBS in close proximity to the LDH layers. A similar result is found for poly(ethylene oxide)/laponite nanocomposites by NMR.[54] On the other hand, the long alkyl tail with the bulky methyl group of the SDBS molecules play the role of plasticizer for the PE segments in the region farer from the LDH sheets. Therefore the high frequency process (process II) is assigned to the PE segments and parts of the alkyl tail of SDBS in a greater distance from the LDH sheets. It should be noted that an increase of the molecular mobility close to exfoliated clay layers was also observed for polypropylene/clay nanocomposites for good dispersed nanoparticles[12] whereas for a bad dispersed system the molecular mobility remains unchanged.

The model function of Havriliak/Negami[55] (HN-function) is used to analyze the β-relaxation region quantitatively. According to the double peak structure the whole fit function consist of two HN-function and reads

$$\varepsilon^*(f) - \varepsilon_\infty = \sum_{k=1,2} \frac{\Delta\varepsilon_k}{(1 + (if/f_k)^{\beta_k})^{\gamma_k}} \qquad (1)$$

f is the frequency ($i = -1^{1/2}$), $f_{0,k}$ is a characteristic frequency related to the frequency of maximal loss $f_{\mathrm{p},i}$ (relaxation rate)[50] of each process, β_k and γ_k are fractional parameters ($0 < \beta \leq 1$ and $0 < \beta\gamma \leq 1$) characterizing the shape of the relaxation time spectra. $\Delta\varepsilon_k$ denotes the dielectric strength of each process. ε_∞ gives ε' for $f \rightarrow \infty$. The relevant details can be found ref 50. To reduce the number of free parameters and to stabilize the fit, $\gamma_i = 1$ (symmetrical loss peaks) is chosen. An example of this analysis is given in Figure 7 for the sample PELDH2 (4.72 wt %) from which the relaxation rates $f_{\mathrm{p},i}$ of each process and the dielectric strength $\Delta\varepsilon_\beta$ of the whole β-relaxation is deduced. For all concentrations of LDH, the β parameter increase with temperature from 0.35 to 0.4 for process I and from 0.4 to 0.55 for process II. An example for this dependency is given in the inset of Figure 8.

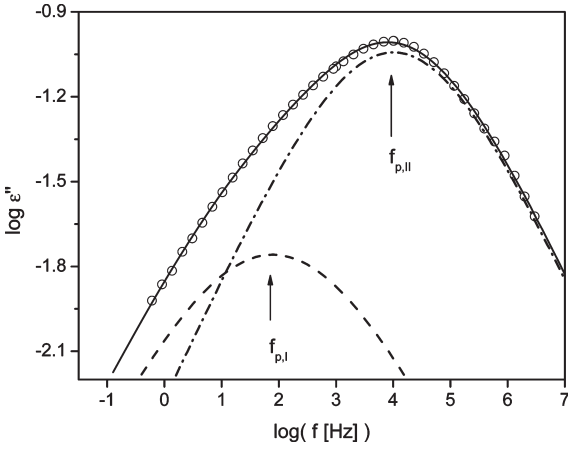

Figure 7. Dielectric loss ε'' versus frequency for the sample PELDH2 (4.72 wt %) at $T = 263.2$ K. The solid line is a fit of two HN-functions to the data. The dashed line is the contribution of the low frequency process where the dashed−dotted line corresponds to that of the high frequency one.

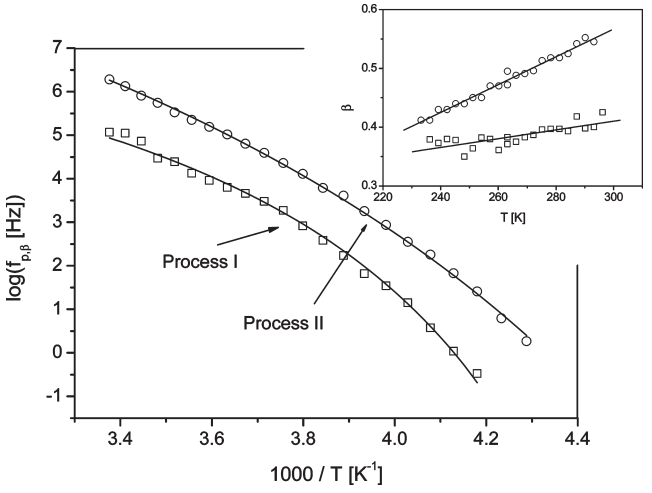

Figure 8. Relaxation rates $f_{p,i}$ vs $1/T$ for the both relaxation processes of the β-relaxation for the sample PELHD6 (16.2 wt %). Lines are fits of the VFT equation to the data as described in the text. The inset gives the temperature dependence of the shape parameter β for the same sample: (□) process I; (○) process II. The lines are linear regressions to the data. The relation of the β-parameter of the HN-function to the Kohlrausch−Williams−Watts β_{KWW} exponent is $\beta \approx \beta_{KWW}{}^{1.23}$. For more details see refs 50 and 57.

Because of the temperature dependence of shape parameter β the β-relaxation processes do not behave thermorheologically simple as also know for other polymers.[32]

The relaxation rates f_p of both processes are plotted versus reciprocal temperature for the sample PELDH6 in Figure 8. For both processes, this trace is curved versus $1/T$, and the data seem to follow the Vogel−Fulcher−Tammann (VFT) equation[56] which reads

$$\log f_p = \log f_\infty - \frac{A}{T - T_0} \qquad (2)$$

(log f_∞, A are constants). T_0 is the so-called Vogel or ideal glass transition temperature. For conventional polymeric systems T_0 is found to be 50 to 70 K below the glass transition temperature T_g. Therefore T_0 can be taken as a measure of T_g.

For a more detailed analysis of the temperature dependence of the relaxation rates a derivative method is applied.[58] This method is sensitive to the functional form of $f_p(T)$

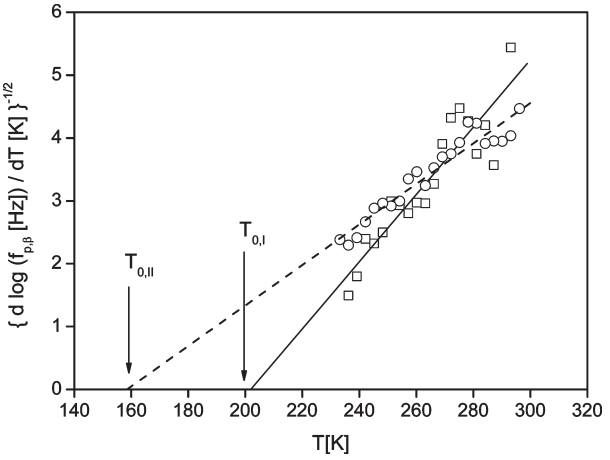

Figure 9. $(d(\log f_{p,\beta})/dT)^{1/2}$ versus temperature for the two different processes PELHD6 (16.2 wt %): (○) high temperature process; (□) low temperature process. The lines are linear regression to the corresponding data sets.

irrespective of the prefactor. For a dependency according to the VFT equation one gets

$$\left[\frac{d(\log f_p)}{dT}\right]^{-1/2} = A^{-1/2}(T - T_0) \qquad (3)$$

In a plot of $[d(\log f_p)/dT]^{-1/2}$ versus T, a VFT behavior shows up as a straight line (see Figure 9). All experimental data can be well described by straight lines which proofs that the temperature dependence of the relaxation rates of both processes is VFT-like. A temperature dependence of the relaxation rates according to the VFT equation is regarded as a sign of glassy dynamics. Therefore it is concluded that both of the observed relaxation processes are due to a dynamic glass transition in spatial regions with different distance to the LDH layers. To have a signature as a glass transition, the spatial extent of these regions should be on the order of 1−3 nm.[59−63] So, it is further concluded that the thickness or the extension of the interfacial region into the bulk matrix is about the same length scale.

To obtain the parameters of the VFT equation the Vogel temperature T_0 was estimated from the derivative technique by linear regression. The parameters log f_∞ and A are obtained by fitting the VFT equation to the corresponding f_p data while keeping T_0 fixed. All parameters are collected in Table 2. An example of this fit is given in Figure 8. This analysis indicates that the temperature dependence of the relaxation rates of the both relaxation processes is quite different characterized by the different slopes of the both regression lines. The difference in the estimated Vogel temperatures is for this LDH concentration around 40 K. So, one has to conclude that the molecular dynamics in the interfacial region around the LDH sheets is quite different. It is worth noting that the value of T_0 found for pure LDPE is in between the values found for the both relaxation processes observed for the nanocomposites.[42]

Figure 5 shows that the temperature position of the β-relaxation of the nanocomposites is independent of the concentration of LDH. This concerns also the temperature dependence of the relaxation rates of the both processes. This indicates that with an increasing content of LDH the relaxation mechanism does not change only the amount of the sensed interfacial region increases. Therefore it can be analyzed by considering all concentrations of LDH

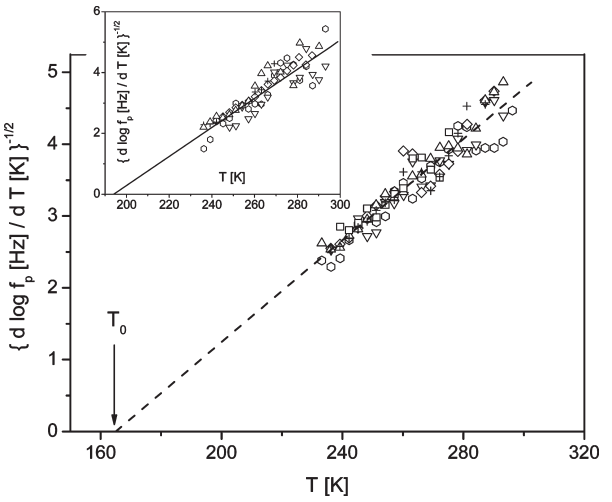

Figure 10. $(d(\log f_{p,\beta})/dT)^{1/2}$ versus temperature for the high frequency processes: (□) 2.43 wt % LDH; (Δ) 4.72 wt % LDH; (+) 6.89 wt % LDH; (◇) 8.94 wt % LDH; (▽) 12.73 wt % LDH; (⬡) 16.2 wt % LDH. The solid line is a linear regression including the data for all concentrations. The inset gives $(d(\log f_{p,\beta})/dT)^{1/2}$ versus temperature for the low frequency processes: (□) 2.43 wt % LDH; (Δ) 4.72 wt % LDH; (+) 6.89 wt % LDH; (◇) 8.94 wt % LDH; (▽) 12.73 wt % LDH; (⬡) 16.2 wt % LDH. The solid line is a linear regression including the data for all concentrations.

simultaneously using the derivative technique (Figure 10). For both processes all data collapse to a single line. To estimate an average value for the Vogel temperatures a linear regression is carried out by using the data for all concentrations of LDH. This procedure increases the statistical relevance of the estimated mean values of T_0 (see Table 2). The difference between both mean Vogel temperatures is 30 K. Using the errors of the slope and the intersection resulting from that joint linear regression a maximal error is calculated for T_0 (see Table 2). For both Vogel temperatures the calculated maximal error is essentially smaller than the difference between the T_0. This statistical analysis confirms that the difference in the temperature dependence of the relaxation rates of both processes and therefore the difference in the molecular mobility in different distances form the LDH sheets. From the VFT parameters a dielectric glass transition temperature can be calculated by $T_g^{Diel} = T(f_p = 10^{-2}\,Hz)$. The average difference in T_g^{Diel} for the both processes is about 10 K.

The Debye theory of dielectric relaxation generalized by Kirkwood and Fröhlich[64] gives for the dielectric relaxation strength

$$\Delta\varepsilon = \frac{1}{3\varepsilon_0} g \frac{\mu^2}{k_B T} \frac{N}{V} \tag{4}$$

where μ is the mean dipole moment related to the process under consideration and N/V is the number density of dipoles involved. Here μ is mainly related to the dipole moment of the SDBS molecule and the number density is related to its concentration, a fact which is well-known for conventional dielectric probe spectroscopy on polyolefins.[42,65] g is the Kirkwood/Fröhlich correlation factor which describes static correlation between the dipoles ($g = 1$, no correlation; $g < 1$, antiparallel orientation; $g > 1$, parallel orientation). k_B is Boltzmann's constant. The Onsager factor describing internal field effects is omitted for the sake of simplicity. ε_0 is the dielectric permittivity of free space. Because of the fact that the estimated dielectric strength for the individual processes of the dynamic glass transition shows a relatively large scatter, only its sum $\Delta\varepsilon_\beta = \Delta\varepsilon_I + \Delta\varepsilon_{II}$, as obtained by the fit of two HN functions, is discussed further. Figure 11 shows the temperature dependence of $\Delta\varepsilon_\beta$ for the nanocomposites. $\Delta\varepsilon_\beta$ decreases with increasing temperature as expected for a dynamic glass transition.[32] As already seen from the raw data (see Figure 5) the dielectric strength of the β-relaxation increases with increasing content of the nanoparticles.

$\Delta\varepsilon_\beta$ is taken at a selected temperature of $T_{Comp} = 263.15$ K and plotted versus the concentration of LDH in Figure 12. For low concentrations of LDH $\Delta\varepsilon_\beta$ varies linearly with c_{LDH} as expected from Equ. 4. This linear dependence proofs that $\Delta\varepsilon_\beta$ is due to the concentration of SDBS molecules. With increasing concentration of LDH the number of the SDBS molecules increases and therefore $\Delta\varepsilon_\beta$. This becomes even clearer from the inset of Figure 12 where the ratio $\Delta\varepsilon_\beta/c_{LDH} \sim g$ is plotted versus the concentration of LDH. For low values of c_{LDH} this ratio is constant in agreement with the simple assumption of an increase of the number density of dipoles. Moreover this linear dependence of $\Delta\varepsilon_\beta$ on the concentration of the nanofiller supports a well exfoliated state of the LDH layers in the polyethylene matrix. Such a behavior will be not characteristic for a microcomposite with embedded unexfoliated larger LDH particles.

For higher values of c_{LDH}, $\Delta\varepsilon_\beta$ increases stronger than expected from a simple increase of the number density of dipoles. This is also confirmed by the step-like increases of the ratio $\Delta\varepsilon_\beta/c_{LDH}$ versus the concentration of the nanofiller (see Figure 12) This points to a change in the structure of the nanocomposites. For higher concentration of the nanofiller the exfoliated LDH sheets cannot be arranged independently from each other. This leads to a correlation or orientation of the LDH sheets giving rise to an increase of the Kirkwood/Fröhlich correlation factor and therefore of $\Delta\varepsilon_\beta$. Of course also an orientation of the exfoliated LDH layers during the extrusion process can take place for higher concentration of LDH. It is worth mentioning again that the temperature dependence of the relaxations rates is not influenced by this structural change.

γ-Relaxation. As discussed above the γ-relaxation in polyethylene corresponds to localized fluctuations within the amorphous regions. For the nanocomposites also a relaxation process in the temperature range of the γ-relaxation is observed. It is analyzed by fitting one Havriliak/Negami model function to the dielectric spectra. From this analysis the relaxation rate $f_{p,\gamma}$ and the dielectric strength $\Delta\varepsilon_\gamma$ are obtained for this process. Like for the β-relaxation a symmetrical fitting function is used ($\gamma_\gamma = 1$). For all concentrations of LDH β-values around 0.2 are obtained, which increases slightly with temperature. Figure 13 gives the relaxation rate of the γ-relaxation versus $1/T$. For all concentrations of LDH the data can be described by an Arrhenius equation

$$f_{p,\gamma} = f_\infty \exp\left(-\frac{E_A}{k_B T}\right) \tag{5}$$

(E_A, activation energy; f_∞, pre-exponential factor). The estimated values are given in Table 2.

The estimated values for the activation energy are around 40 kJ/mol and seem to be independent of the concentration of the LDH. These values are in agreement with a localized relaxation process. The absolute value of the relaxation rate slightly depends on the concentration of the nanofiller. With increasing concentration of LDH $f_{p,\gamma}$ increases and saturates for high concentrations of LDH (see Figure 13). It is worth noting that the value where $f_{p,\gamma}$ reaches the plateau is approximately the same where the concentration

Table 2. Estimated VFT Parameters for the β-Relaxation and Activation Parameters for the γ-Relaxation As Described in the Text[a]

	β-relaxation							
	low frequency process			high frequency process			γ-relaxation	
sample	log(f_∞[Hz])	A [K]	T_0 [K]	log(f_∞[Hz])	A [K]	T_0 [K]	log(f_∞[Hz])	E_A [kJ/mol]
PELDH1				12.2	840.0	158.9	14	37.6
PELDH2	8.8	371.3	194.7	11.8	716.8	169.0	14.0	37.9
PELDH3	8.1	274.4	202.1	11.9	720.5	168.8	14.3	38.2
PELDH4	9.5	405.5	193.7	12.0	739.4	167.2		
PELDH5	10.1	440	198.7	12.7	810.9	168.0	14.1	36.1
PELDH6	8.6	346.8	201.9	13.2	957.3	158.5	14.3	36.9
mean value			194 ± 15			165 ± 10		

[a] For the sample PELDH1 the separation of β-relaxation cannot be done unambiguously. The mean values of T_0 are estimated using a linear regression of all data for that relaxation process. The given errors are maximal errors which are calculated using the errors of the slope and the section of this regression line.

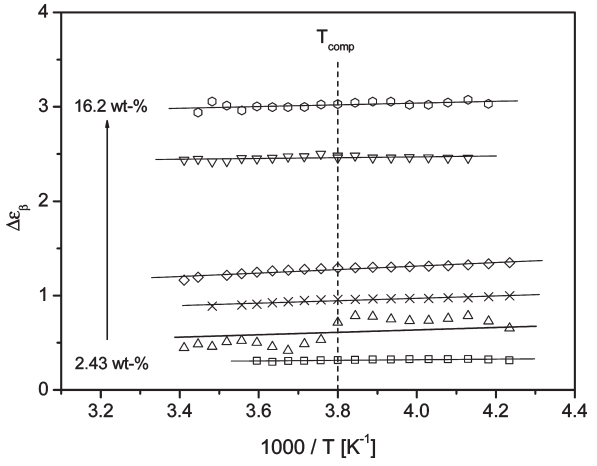

Figure 11. Dielectric relaxation strength $\Delta\varepsilon_\beta$ for the β-relaxation vs 1/T for the different nanocomposites: (□) 2.43 wt % LDH; (Δ) 4.72 wt % LDH; (+) 6.89 wt % LDH; (◇) 8.94 wt % LDH; (▽) 12.73 wt % LDH; (⬡) 16.2 wt % LDH. The solid lines are linear regressions to the corresponding data sets. The dashed lines indicate the temperature for comparison.

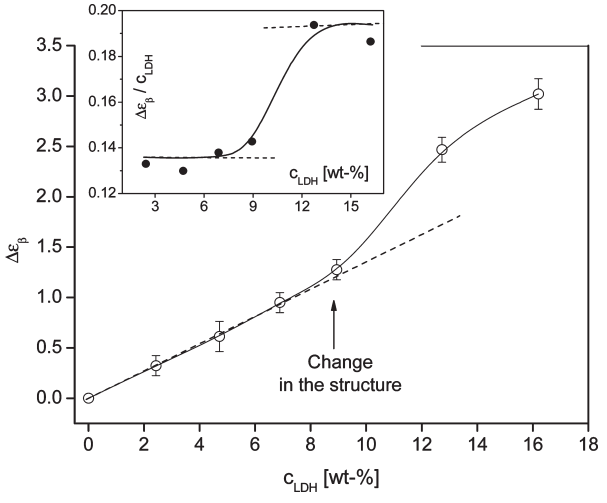

Figure 12. Dielectric relaxation strength $\Delta\varepsilon_\beta$ vs the concentration of LDH at T_{Comp} = 263.15 K. The solid line is a guide to the eyes. The dashed lines indicates the linear behavior $\Delta\varepsilon_\beta \sim c_{LDH}$. The inset gives the ratio $\Delta\varepsilon_\beta/c_{LDH}$ vs the concentration of LDH. The solid line is a guide to the eyes.

dependence of $\Delta\varepsilon_\beta$ also changes (compare Figure 12). The γ-relaxation is due to localized fluctuations in the amorphous regions of polyethylene. With increasing LDH content the absolute fraction of the interfacial region increases which is also amorphous. As discussed above a part of this

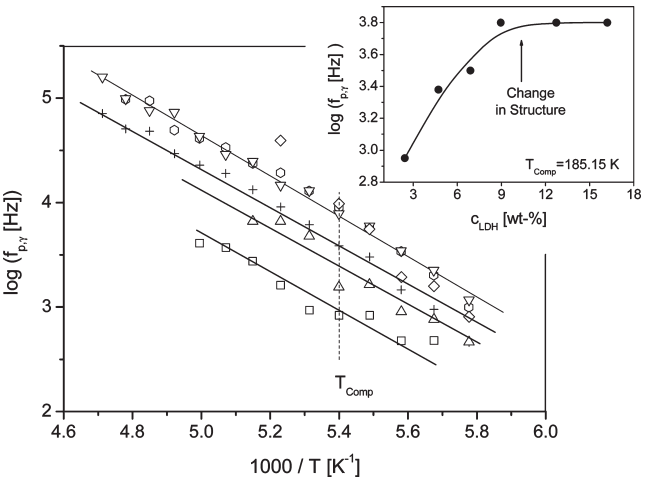

Figure 13. Relaxation rates $f_{p,\gamma}$ vs $1/T$ for the γ-relaxation for the nanocomposites: (□) 2.43 wt % LDH; (Δ) 4.72 wt % LDH; (+) 6.89 wt % LDH; (◇) 8.94 wt % LDH; (▽) 12.73 wt % LDH; (⬡) 16.2 wt % LDH. The solid lines are fits of the Arrhenius equation to the corresponding data. The inset give $f_{p,\gamma}$ vs c_{LDH} at T = 185.15 K. The solid line is a guide to the eyes.

interfacial region is plasticized by the long alkyl tails of the SDBS molecules and has probably a decreased density compared to bulk LDPE. In these regions, the localized fluctuations can take place more easily and should have lower activation energies. The shape of loss peak of the γ-relaxation is due to a broad distribution of activation energies.[32] With increasing LDH content in this distribution, the contribution of the low activation energies increases and the mean value of the relaxation rate shifts slightly to higher values.

Figure 14 gives the temperature dependence of the dielectric relaxation strength $\Delta\varepsilon_\gamma$ of the γ-relaxation for the nanocomposites. With increasing content of the nanofiller $\Delta\varepsilon_\gamma$ increases (see Figure 15). Keeping in mind that the γ-relaxation is due to localized fluctuations in the amorphous regions of PE. As discussed above with increasing content of LDH the degree of crystallization decreases and therefore the relative amount of the amorphous phase increases. This line of argumentation is supported by the linear dependence of $\Delta\varepsilon_\gamma$ with the c_{LDH} (see Figure 15). Taking the ratio $\chi = \Delta H_{Melt}/\Delta H_{Melt}(c_{LDH} = 0)$ (enthalpy values normalized to the content of the polymer) as a crude estimation for the degree of crystallization in the inset of Figure 15 $\Delta\varepsilon_\gamma$ is plotted versus χ. $\Delta\varepsilon_\gamma$ decreases linearly with χ and becomes approximately zero for $\chi = 1$. This confirms once again the hypothesis that the γ-relaxation is taking place in the amorphous regions of the polymer matrix.

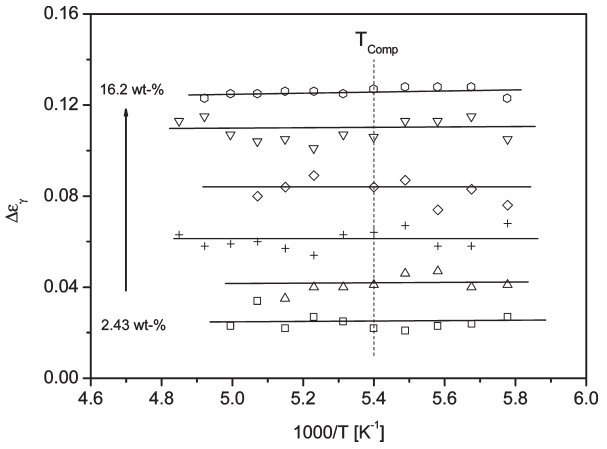

Figure 14. Dielectric relaxation strength $\Delta\varepsilon_\gamma$ for the γ-relaxation vs 1/T for the different nanocomposites: (□) 2.43 wt % LDH; (Δ) 4.72 wt % LDH; (+) 6.89 wt % LDH; (◇) 8.94 wt % LDH; (▽) 12.73 wt % LDH; (⬡) 16.2 wt % LDH. The solid lines are guides for the eyes.

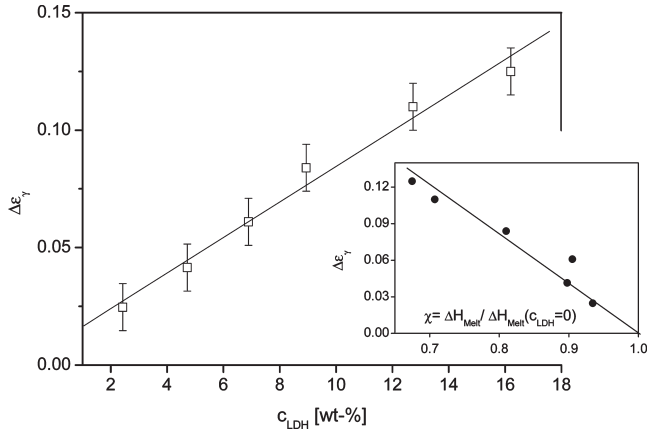

Figure 15. Dielectric relaxation strength $\Delta\varepsilon_\gamma$ for the γ-relaxation vs the concentration of LDH at T_{Comp} = 185.15 K. The line is a linear regression to the data. The inset gives $\Delta\varepsilon_\gamma$ versus $\chi = \Delta H_{Melt}/\Delta H_{Melt}(c_{LDH} = 0)$ (enthalpy values normalized to the content of the polymer). The line is a guide for the eyes.

Interfacial Polarization. For the nanocomposites, an additional process is observed at higher temperatures than the melting temperature (see Figure 16). This peak is assigned to an interfacial polarization process[50] (Maxwell/Wagner/Sillars) due to the blocking of charge carriers at internal phase boundaries. Generally, such an interfacial polarization process is caused by (partial) blocking of charge carriers at internal surfaces or interfaces of different phases having different values of the dielectric permittivity and/or conductivity at a mesoscopic length scale or at electrodes.

Although an interfacial polarization is not a relaxation process, it can be also described by fitting the HN function to the data (see Figure 16) and a characteristic frequency $f_{Inter} \sim 1/\tau_{Inter}$ can be deduced. With increasing concentration of the nanofiller, the interfacial process shifts to higher frequencies at a fixed temperature (see Figure 16). This becomes even clearer considering the temperature dependence of f_{Inter} (see Figure 17). Because of this shift, the different temperature dependencies of f_{Inter} for the different concentrations of nanofiller and the fact that all samples have approximately the same thickness electrode polarization could be excluded. Moreover, the interfacial process can be also observed at temperatures above T_M. Therefore also the blocking of charge carriers at lamellar boundaries is exscluded. Considering the predominantly exfoliated geometry of the

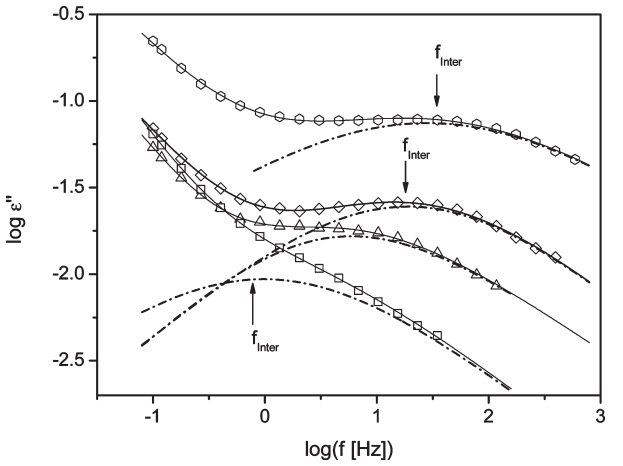

Figure 16. Dielectric loss ε'' versus frequency at T = 413.15 K for different nanocomposites: (□) 2.43 wt % LDH; (Δ) 4.72 wt % LDH; (◇) 8.94 wt % LDH; (⬡) 16.2 wt % LDH. The solid lines are fit of the HN-function to the data including a conductivity contribution. The dashed−dotted lines are the contributions of the interfacial process to the dielectric loss.

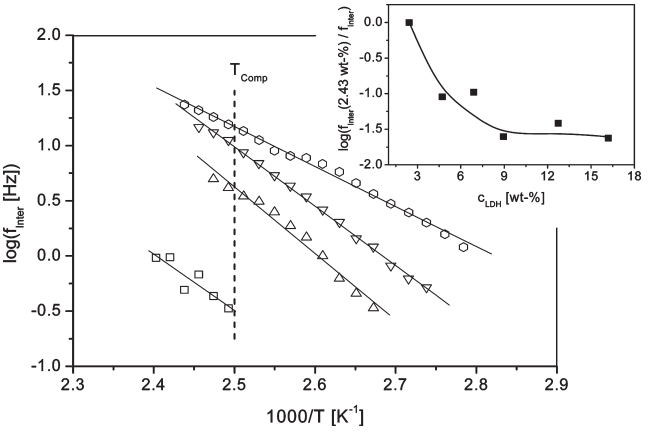

Figure 17. Temperature dependence of the characteristic frequency f_{Inter} of the interfacial process vs $1/T$ for different nanocomposites: (□) 2.43 wt % LDH; (Δ) 4.72 wt % LDH; (▽) 12.73 wt % LDH; (⬡) 16.2 wt % LDH. The solids lines are fits of the Arrhenius equation to the data. The inset gives the dependence of the characteristic rate of the interfacial polarization versus concentration of LDH reduced by the rate of the sample with 2.43 wt % LDH at T_{Comp} = 400 K. This ratio is proportional to $\sim d/d$(2.43 wt %). The solid line is a guide for the eyes.

LDH sheets dispersed in the polymer matrix this process is related of the blocking of charge carriers at internal polymer/LDH interfaces. The shift of f_{Inter} at fixed temperature to higher values with increasing concentration of LDH can be understood that with increasing concentration of the nanofiller the mean distance d between the exfoliated LDH layers becomes smaller, and so the charge carriers need a shorter time to diffuse between them before being blocked at the internal phase boundary. This can be quantitatively discussed in an oversimplified model. If d roughly characterizes the mean distance between exfoliated LDH layers the blocking of the charge carriers at these walls is described by an electrical double layer with an effective spacing characterized by its Debye length L_D. This double layer represents an additional capacitance C_{DL} in the system and the time-dependence of the polarization is due to the charging/discharging of that electrical double layer. The time constant τ_{Inter} for this process can be estimated in the simplest possible approach analogous to that for electrode polarization[50] and is related to the conductivity σ of the polymeric matrix.

Considering the conductivity to be inversely proportional to the mean distance $\sigma \sim \sigma_0/d$, one obtains

$$\tau_{\text{Inter}} = \frac{C_{\text{DL}}}{\sigma} \approx \frac{\varepsilon_S \varepsilon_0}{\sigma_0} \frac{d}{2L_D} \quad (6)$$

ε_S is the permittivity and σ_0 is the specific dc-conductivity of the matrix. Assuming further that ε_S, σ_0, and L_D depend only weakly on the overall LDH concentration, the relative change of the mean distance between the LDH sheets with the concentration of the nanofiller can be estimated to be

$$\frac{\tau_{\text{Inter},1}}{\tau_{\text{Inter},2}} = \frac{f_{\text{Inter},2}}{f_{\text{Inter},1}} \approx \frac{d_1}{d_2} \quad (7)$$

from the data shown in Figure 17. A similar approach was discussed in[12] for silicate layers dispersed in a modified polypropylene matrix. The relative change in the distance between the LDH sheets is calculated according to eq 7 and plotted versus the concentration of LDH in the inset of Figure 17. With increasing c_{LDH}, the distance of the LDH layers decreases. Therefore, an analysis of the Maxwell/Wagner/Sillars polarization provides a handy tool for a rough estimation of the degree of dispersion of the nanoparticles in polymer based nanocomposites.[12,19]

The difference in the temperature dependences of the characteristic frequencies of the interfacial process can be understood as follows. The Maxwell/Wagner/Sillars polarization is investigated in the molten state of polyethylene. In that state the polymer chain have a high mobility and the exfoliated LDH sheets are able to aggregate. Depending on the temperature and the concentration of the nanofiller this aggregation phenomena can be different which causes the different temperature dependence of f_{Inter}.

Conclusion

Nanocomposites are prepared in a two-step procedure by melt mixing of polyethylene and layered doubled hydroxides (LDH), where maleic anhydride grafted polyethylene is used as compatibilizer. LDH have been modified by sodium dodecylbenzene sulfonate (SDBS) as a surfactant. Previous investigations show that the synthesized nanocomposites have a predominantly exfoliated morphology.[21]

The thermal properties of the nanocomposites are investigated by differential scanning calorimetry. Both the melting and crystallization enthalpies decrease with increasing concentration of LDH. Reduced to the content of the polymer the phase transition enthalpies ΔH_{Norm} decreases linearly with the concentration of the nanofiller. The extrapolation of ΔH_{Norm} to zero leads to a limiting concentration of ca. 50 wt % LDH, where the crystallization should be completely suppressed by the presence of the nanoparticles.

The dielectric loss of pure polyethylene is weak but several relaxation processes can be indentified:[32] a γ-process at low temperatures which corresponds to localized fluctuations in the amorphous parts of polyethylene and a β-relaxation which corresponds to the dynamic glass transition due to cooperative segmental fluctuations. At even higher temperatures, a further process takes place which is related to molecular fluctuations in the crystalline phase.

The intensity of the β-relaxation (dynamic glass transition) increases strongly with increasing concentration of LDH for the nanocomposites. This increase in the dielectric relaxation strength of the dynamic glass transition is related to the increase in the concentration of the quite polar SDBS surfactant molecules which increases with the concentration of LDH. The surfactants are adsorbed onto the LDH layers and its alkyl tails form a common phase with the polyethylene segments close the nanoparticles. Therefore a detailed investigation of the β-relaxation provides information about the molecular mobility and structure in the interface area between the LDH layers and the matrix polymer. It was shown that the peak of the β-relaxation consist of two processes. These processes are assigend to regions of different molecular mobility in different distances to the LDH nanofillers. The temperature dependence of the relaxation rates of both processes follows the Vogel−Fulcher−Tammann formula which indicates glassy dynamics. The difference in the corresponding glass temperatures measured by the ideal glass transition or Vogel temperature T_0 is about 30 K. The low frequency component of the β-relaxation of the nanocomposites is assigned to polyethylene segments in a close proximity of the LDH because the SDBS molecules are strongly adsorbed at the surfaces of the nanofiller and have therefore a strongly reduced molecular mobility. The high frequency process of the β-relaxation is related to polyethylene segments is in a farer distance form the LDH layers. The higher molecular mobility is caused by a plasticization of the alkyl tail of the SDBS surfactants terminated with a methyl group.

The dielectric strength $\Delta\varepsilon_\beta$ of the β-relaxation increases with increasing concentration of LDH. Up to ca. 8 wt % of LDH the dependence of $\Delta\varepsilon_\beta$ on c_{LDH} is linear as predicted by the Debye formula. For higher concentration than 8 wt % $\Delta\varepsilon_\beta$ increases much stronger than expected from the Debye theory of dielectric relaxation. This is interpreted by increasing correlation of the exfoliated LDH layers with increasing concentration of LDH.

The temperature dependence of the relaxation rates of the γ-relaxation follows the Arrhenius equation with an activation energy of around 40 kJ/mol independent of the concentration of LDH. The relaxation strength of the γ-process increases with the concentration of the nanofiller. Because the γ-relaxation is related to localized fluctuation in the amorphous regions of polyethylene, it is concluded that the content of the amorphous phase increases with increasing concentration of LDH. This is confirmed by a linear dependence of $\Delta\varepsilon_\gamma$ on the roughly estimated degree of crystallization.

For the nanocomposite systems a distinct high temperature process was observed which is due to Maxwell−Wagner-Sillars-polarization because charge carriers can be blocked at the exfoliated LDH layers. Corresponding time constants allow a rough estimate of characteristic length scales in the nanocomposites and therefore also depend on the degree of dispersion of the filler particles. This correlation may provide a possible route for the development of testing or monitoring procedures in the field of nanocomposite formation.

Acknowledgment. F.R.C. thanks the German Academic Exchange Service (DAAD) for financial support. Mr. N. Neubert (BAM) is thanked for the DSC measurements.

References and Notes

(1) LeBaron, P. C.; Wang, Z.; Pinnavaia, T. J. *Appl. Clay Sci.* **1999**, *15*, 11.
(2) Novak, B. M. *Adv. Mater.* **1993**, *5*, 422.
(3) Alexandre, M.; Dubois, P. *Mater. Sci. Eng.* **2000**, *28*, 1.
(4) Krishnamoorti, R.; Vaia, R. A. *Polymer Nanocomposites*; ACS Symposium Series 804; American Chemical Society: Washington, DC, 2002.
(5) Sinha Ray, S.; Okamoto, M. *Prog. Polym. Sci.* **2003**, *28*, 1539.
(6) Nalwa, H. S. *Handbook of Organic-Inorganic Hybrid Materials and Nanocomposites*; American Scientific Publishers: Stevenson Ranch, CA, 2003; Vol. 2.
(7) Leuteritz, A.; Kretzschmar, B.; Pospiech, D.; Costa, R. F.; Wagenknecht, U.; Heinrich, G. Industry-relevant preparation, characterization and applications of polymer nanocomposites. In: *Polymeric nanostructures and their applications*; Nalwa, H. S., Ed.; American Scientific Publishers: Los Angeles, 2007.

(8) Vaia, R. A.; Giannelis, E. P. *MRS Bull*. **2001**, *26*, 394.
(9) Davis, S. R.; Brough, A. R.; Atkinson, A. *J. Non-Cryst. Solids* **2003**, *315*, 197.
(10) Fragiadakis, D.; Pissis, P.; Bokobza, L. *Polymer* **2005**, *46*, 6001.
(11) Hooper, J. B.; Schweitzer, K. S. *Macromolecules* **2005**, *38*, 8850.
(12) Böhning, M.; Goering, H.; Fritz, A.; Brzezinka, K. W.; Turky, G.; Schönhals, A.; Schartel, B. *Macromolecules* **2005**, *38*, 2764.
(13) Heilmann, A. *Polymer Films with Embedded Metal Nanoparticles*; Springer: Berlin, 2003.
(14) Xie, X. L.; Mai, Y. W.; Zhou, X. P. *Mater. Sci. Eng. Res.* **2005**, *49*, 89.
(15) Bernholc, J.; Brenner, D.; Nardelli, M. B.; Meunier, V.; Roland, C. *Annu. Rev. Mater. Res.* **2002**, *32*, 347.
(16) Moniruzzaman, M.; Winey, K. I. *Macromolecules* **2006**, *39*, 5194.
(17) Lichtenhan, J. D.; Schwab, J. J.; Reinerth, W. A. *Chem. Innov.* **2001**, *31*, 3.
(18) Joshi, M.; Butola, B. S. *J. Macromol. Sci. B: Polym. Rev.* **2004**, *C44*, 389.
(19) Hao, N.; Böhning, M.; Goering, H.; Schönhals, A. *Macromolecules* **2007**, *40*, 2955.
(20) Hao, N.; Böhning, M.; Schönhals, A. *Macromolecules* **2007**, *40*, 9672.
(21) Costa, F. R.; Saphiannikova, M.; Wagenknecht, U.; Heinrich, G. *Adv. Polym. Sci.* **2008**, *210*, 101.
(22) Costa, F. R.; Abdel-Goad, M.; Wagenknecht, U.; Heinrich, G. *Polymer* **2005**, *46*, 4447.
(23) Costa, F. R.; Wagenknecht, U.; Jehnichen, D.; Abdel-Goad, M.; Heinrich, G. *Polymer* **2006**, *47*, 1649.
(24) Tichit, D.; Coq, B. *Cattech* **2003**, *7*, 206.
(25) Frunza, L.; Schönhals, A.; Frunza, S.; Parvulescu, V. I.; Cojocaru, B.; Carriazo, D.; Martín, C.; Rives, V. *J. Phys. Chem. A* **2007**, *111*, 5166.
(26) van der Ven, L.; Van Gemert, M. L. M.; Batenburg, L. F.; Keern, J. J.; Gielgens, L. H.; Koster, T. P. M.; Fischer, H. R. *Appl. Clay Sci.* **2000**, *17*, 25.
(27) Du, L.; Qu, B.; Zhang, M. *Polym. Degrad. Stab.* **2007**, *92*, 497.
(28) Anastasiadis, S. H.; Karatasos, K; Vlachos, G.; Manias, E.; Gianneis, E. P. *Phys. Rev. Lett.* **2000**, *84*, 915.
(29) Schwartz, G. A.; Bergman, R.; Swenson, J. *J. Chem. Phys.* **2004**, *120*, 5736.
(30) Mijovic, J.; Lee, H. K.; Kenny, J.; Mays, J. *Macromolecules* **2006**, *39*, 2172.
(31) Elmahdy, M. M.; Chrissopoulou, K.; Afratis, A.; Floudas, G.; Anastasiadis, S. H. *Macromolecules* **2006**, *39*, 5170.
(32) Schönhals, A. Molecular Dynamics in Polymer Model Systems. In *Broadband Dielectric Spectroscopy*, Kremer, F., Schönhals, A., Eds.; Springer: Berlin, 2002; p 225.
(33) Kremer, F.; Schönhals, A. Broadband Dielectric Measurement Techniques. In *Broadband Dielectric Spectroscopy*; Kremer, F., Schönhals, A., Eds.; Springer: Berlin, 2002; p 35.
(34) Wunderlich, B. *J. Chem. Phys.* **1962**, *37*, 2429.
(35) Sworen, J. C.; Wagener, K. B.; Baugh, L. S.; Rucker, S. P. *J. Am. Chem. Soc.* **2003**, *125*, 2228.
(36) Crist, B.; Howard, P. R. *Macromolecules* **1999**, *32*, 3057.
(37) Schick, C.; Wurm, A. Personal communication.
(38) Homminga, D.; Goderis, B.; Dolbnya, I.; Groeninckx, G. *Polymer* **2006**, *47*, 1620.
(39) Miltner, H. E.; Grossiord, N.; Lu, K.; Loos, J.; Koning, C. E.; van Mele, B. *Macromolecules* **2008**, *41*, 5753.
(40) McCrum, N. G.; Read, B. E.; Williams, G. *Anelastic and Dielectric Effects in Polymeric Solids*; Wiley: New York, 1967 (Reprinted by Dover 1991).
(41) Frübing, P.; Blischke, D.; Gerhard-Multhaupt, R.; Khalil, M. S. *J. Phys. D: Appl. Phys.* **2001**, *34*, 3051.
(42) van den Berg, O.; Sengers, W. G. F.; Jager, W. F.; Picken, S. J.; Wübbenhorst, M. *Macromolecules* **2004**, *37*, 2460.
(43) Mansfield, M.; Boyd, R. *J. Polym. Sci. Phys. Ed.* **1978**, *16*, 1227.
(44) Schmidt-Rohr, K.; Spiess, H. W. *Macromolecules* **1991**, *24*, 5288.
(45) Hu, W. G.; Boeffel, C.; Schmidt-Rohr, K. *Macromolecules* **1999**, *32*, 1611.
(46) Ascraft, C. R.; Boyd, R. *J. Polym. Sci. Phys. Ed.* **1976**, *14*, 2153.
(47) van den Berg, O.; Wübbenhorst, M.; Picken, S. J.; Jager, W. F. *J. Non-Cryst. Solids* **2005**, *351*, 2694.
(48) Schönhals, A. Molecular Dynamics in Polymer Model Systems. In *Broadband Dielectric Spectroscopy*; Kremer, F., Schönhals, A., Eds.; Springer: Berlin, 2002; p 225.
(49) van Turnhout, J.; Wübbenhorst, M. *Dielectric Newsletter, Issue November*; NOVOCONTROL GmbH: Hundsangen, Germany, 2000.
(50) Schönhals, A.; Kremer, F. Analysis of Dielectric Spectra. In *Broadband Dielectric Spectroscopy*; Kremer, F., Schönhals, A., Eds.; Springer: Berlin, 2002; p 59.
(51) Jacobs, J. D.; Koerner, H.; Heinz, H.; Farmer, B. L.; Mirau, P.; Garrett, P. H.; Vaia, R. A. *J. Phys. Chem. B* **2006**, *110*, 20143.
(52) Kubies, D.; Jérôme, R.; Grandjean, J. *Langmuir* **2002**, *18*, 6159.
(53) Brás, A. R.; Dionísio, M.; Schönhals, A. *J. Phys. Chem. B* **2008**, *112*, 8227.
(54) Lorthioir, C.; Lauprêtre, F.; Soulestin, J.; Lefebvre, J.-M. *Macromolecules* **2009**, *42*, 218.
(55) (a) Havriliak, S.; Negami, S. *Polymer* **1967**, *8*, 161. (b) Havriliak, S.; Negami, S. *J. Polym. Sci. C* **1966**, *16*, 99.
(56) (a) Vogel, H. *Phys. Z.* **1921**, *22*, 645. (b) Fulcher, G. S. *J. Am. Ceram. Soc.* **1925**, *8*, 339. (c) Tammann, G.; Hesse, W. *Z. Anorg. Allg. Chem.* **1926**, *156*, 245.
(57) Alavarez, F.; Alegria, A.; Colmenero, J. *Phys. Rev. B* **1991**, *73*, 3348.
(58) Kremer, F.; Schönhals, A. The Scaling of the Dynamics of Glasses and Supercooled Liquids Spectra. In *Broadband Dielectric Spectroscopy*; Kremer, F., Schönhals, A., Eds.; Springer: Berlin, 2002; p 99.
(59) Donth, E. *J. Non-Cryst. Solids* **1982**, *53*, 325.
(60) Hempel, E.; Hempel, G.; Hensel, A.; Schick, C.; Donth, E. *J. Phys. Chem. B* **2000**, *104*, 2460.
(61) Sills, S.; Gray, T.; Overney, R. M. *J. Chem. Phys.* **2005**, *123*, 134902.
(62) Berthier, L.; Biroli, G.; Bouchaud, J. P.; Cipelletti, L.; El Masri, D.; L'Hote, D.; Ladieu, F.; Pierno, M. *Science* **2005**, *310*, 1797.
(63) Cangialosi, D.; Alegria, A.; Colmenero, J. *Phys. Rev. E* **2007**, *76*, 011514.
(64) Schönhals, A.; Kremer, F. Theory of Dielectric Relaxation Spectra in Broadband Dielectric Spectroscopy. In *Broadband Dielectric Spectroscopy*; Kremer, F., Schönhals, A., Eds.; Springer: Berlin, 2002; p 1.
(65) Kessairi, K.; Napolitano, S.; Capaccioli, S.; Rolla, R.; Wübbenhorst, M. *Macromolecules* **2007**, *40*, 1786.
(66) Alavarez, F.; Alegria, A.; Colmenero, J. *Phys. Rev. B* **1991**, *73*, 3348.